Kinematic wave computation using an efficient implicit method

Ming-Hseng Tseng

ABSTRACT

The kinematic wave theorem is the simplest and widely employed distributed routing method used in practical applications for the computation of flood wave propagation in overland and open-channel flows with steep topography. In this paper, an efficient finite-difference implicit MacCormack scheme is developed for the simulation of one-dimensional kinematic wave flows. Simulated results are compared with two analytical solutions and one experimental measurement to assess the performance of an explicit MacCormack scheme, implicit nonlinear kinematic wave scheme and implicit MacCormack scheme. The computed results show that the proposed implicit MacCormack scheme is simple, accurate, highly stable and greatly efficient in solving kinematic wave problems.

Key words | channel flow, explicit MacCormack scheme, implicit MacCormack scheme, implicit nonlinear kinematic wave scheme, kinematic wave, overland flow

Ming-Hseng Tseng
School of Applied Information Sciences,
Chung Shan Medical University,
No. 110, Sec. 1, Jian-Koa N. Road,
402 Taichung,
Taiwan
Tel.: +886 4 2473 0022 17195
Fax: +886 4 2473 0022 17190
E-mail: *mht@csmu.edu.tw*

INTRODUCTION

The flow of water through the soil and stream channels of a watershed is a distributed process because the flow rate, velocity and depth vary in the space throughout the watershed. Estimates of the flow rate or water level at important locations in the channel system can be obtained using a distributed flow routing model (Chou *et al.* 1988). Distributed flow routing models can be used to describe the transformation of storm rainfall into runoff over a watershed. This, in turn, can produce a flow hydrograph for the watershed outlet. This hydrograph becomes the input at the upstream end of a river or pipe system routed to the downstream end. For many practical purposes, the spatial variation in velocity across the channel with respect to depth can be ignored. This way, the variation of the flow process can be isolated only in the main direction of the flow along the channel.

Flood wave propagation in overland and channel flows may be described by complete equations of motion for unsteady nonuniform flow, known as dynamic wave equations. This was first proposed by Barre de Saint-Venant in 1871. Due to the fact that dynamic wave equations involve a high degree of complexity in computation, the Saint-Venant equations have been simplified. Several simplified forms are being used to efficiently implement the approximate wave models. Under a different set of simplifying assumptions, all distributed flow routing models can be classified into the kinematic wave, the diffusion wave, the quasi-steady dynamic wave and the full dynamic wave models. The simplest distributed model is the kinematic wave model, which neglects local acceleration, convective acceleration and pressure terms in the momentum equation; that is, it assumes that the friction and gravity forces balance each other. In cases where the bed slope is dominant in the momentum equation, most flood waves behave as kinematic waves. Previous studies (Lighthill & Whitham 1955; Henderson 1966) have proven that the velocity of the main part of a natural flood wave approximates that of a kinematic wave in steep rivers

doi: 10.2166/hydro.2010.068

(bed slope $>$ 0.002). The one-dimensional kinematic wave model can be used to simulate these overland and open-channel flows (Lighthill & Whitham 1955; Freeze 1978; Cundy & Tento 1985; Chou *et al.* 1988; Singh 1996).

Numerous explicit and implicit finite-difference schemes have been widely used (Cunge *et al.* 1980; Chou *et al.* 1988) to solve different distributed flow routing models. Several advantages of the explicit MacCormack (EMAC) scheme make the method a popular choice in computational hydraulics. Firstly, the scheme is a shock-capturing technique with a second-order accuracy both in time and space. Secondly, the inclusion of the source terms is relatively simple. Thirdly, it is suitable for implementation in an explicit time-marching algorithm. Tseng & Chu (2000) investigated the accuracy of four different versions of the total variation diminishing (TVD) MacCormcak explicit scheme. Tseng & Wang (2004) discovered that the explicit MacCormack model, when compared with the TVD-MacCormack, may be a superior choice for simulating subcritical flows with strong bed topography variations. This was proven by discretizing the source terms at each step with forward or backward difference, in the same manner as the flux gradient. Kazezyılmaz-Alhan *et al.* (2005) studied the reliability of the explicit MacCormack, explicit linear, implicit nonlinear and the four-point implicit schemes for solving one-dimensional overland flows. Under the Courant–Friedrich–Lewy (CFL) stability condition, they concluded that the explicit MacCormack method should be generally preferred as a solution technique over the explicit linear and implicit methods for solving overland flow problems.

This paper proposes a robust implicit MacCormack (IMAC) scheme to be used in the construction of a simple, accurate and efficient solver for kinematic wave computations. The performance of the proposed method will be tested against the traditional EMAC scheme and the widely used implicit nonlinear kinematic wave (INKW) scheme. All these schemes, including the proposed one, will be used to solve overland and channel flow problems. The comparative results will be presented.

None of the previous studies have reported the results of the use of the implicit MacCormack scheme to calculate kinematic wave flows. This paper, therefore, is the first attempt to explore the potential of the proposed method for one-dimensional overland and channel flow routing. In the following sections, the formulations of the proposed approach are defined, the numerical testing scenarios are described, and the stability, accuracy and efficiency of these schemes are compared and evaluated.

GOVERNING EQUATIONS

Based on the hydrostatic pressure distribution and small channel slope assumptions, an unsteady open-channel flow can be described by Saint-Venant Equations (Chou *et al.* 1988). The shallow water flows can be presented in a conservative form for continuity (Equation (1)) and momentum (Equation (2)) as

$$\frac{\partial A}{\partial t}+\frac{\partial Q}{\partial x}=q_l \tag{1}$$

$$\frac{\partial Q}{\partial t}+\frac{\partial(\beta Q^2/A)}{\partial x}+gA\frac{\partial y}{\partial x}=gA(S_o-S_f)+\beta q_l v_x \tag{2}$$

where t represents the time, x is the longitudinal distance along a channel, A is the wetted cross-sectional area, Q is the flow rate volume, q_l is the lateral inflow rate, β is the momentum correction factor, g is the gravitational acceleration, y is the water depth, S_o is the bed slope, S_f is the friction slope and v_x is the lateral inflow velocity.

The momentum equation consists of six terms responsible for the physical processes that govern the flow momentum. These terms are the local acceleration term, the convective acceleration term, the pressure force term, the gravity force term, the friction force term and the lateral inflow force term. The local and convective acceleration terms represent the effect of inertial forces on the flow. For a kinematic wave, the acceleration and the pressure terms in the momentum equation are negligible. Therefore, the wave motion can be described principally by the equation of continuity. The kinematic wave model is defined by the following Equations (Chou *et al.* 1988):

$$\frac{\partial A}{\partial t}+\frac{\partial Q}{\partial x}=q_l \tag{3}$$

$$A=\alpha Q^{\beta} \tag{4}$$

For example, the Manning equation written with $S_o = S_f$ and $R = A/P$ is

$$A = \left(\frac{nP^{2/3}}{c_I S_o^{1/2}}\right)^{3/5} Q^{3/5} \tag{5}$$

where n denotes the Manning roughness coefficient and P represents the wetted perimeter where c_I is 1 for SI units and 1.49 for British units.

By differentiating Equation (5) and substituting it into Equation (3), the result will be

$$\frac{\partial Q}{\partial x} + \alpha\beta Q^{\beta-1}\frac{\partial Q}{\partial t} = q_l \tag{6}$$

The characteristic equations for a kinematic wave can be derived from Equation (6) as

$$\frac{\mathrm{d}Q}{\mathrm{d}x} = q_l \tag{7}$$

$$c_k = \frac{\mathrm{d}x}{\mathrm{d}t} = \frac{1}{\alpha\beta Q^{\beta-1}} = \frac{\mathrm{d}Q}{\mathrm{d}A} \tag{8}$$

where c_k is the kinematic wave celerity. This implies that an observer moving at a velocity of c_k with the flow would see the flow rate increasing at a rate of q_l.

NUMERICAL APPROACHES

The computational domain is discretized as $x_i = i\Delta x$ and $t^j = j\Delta t$, where Δx is the size of a uniform mesh and Δt is the time increment. The performances of the three finite-difference schemes are investigated in this study. These schemes include the widely used INKW scheme, the traditional EMAC scheme and the proposed IMAC scheme.

Nonlinear implicit scheme

The implicit nonlinear finite-difference formulation of kinematic wave Equations (Li *et al.* 1975), denoted as the INKW scheme, can be expressed as

$$\begin{cases} f\left(Q_{i+1}^{j+1}\right) = \frac{\Delta t}{\Delta x} Q_{i+1}^{j+1} + \alpha\left(Q_{i+1}^{j+1}\right)^{\beta} - C \\ C = \frac{\Delta t}{\Delta x} Q_i^{j+1} + \alpha\left(Q_{i+1}^{j}\right)^{\beta} + 0.5\Delta t\left(q_{l_{i+1}}^{j+1} + q_{l_{i+1}}^{j}\right) \end{cases} \tag{9}$$

where $f(Q_{i+1}^{j+1})$ represents a nonlinear function of the unknown flow rate Q_{i+1}^{j+1}. Equation (9) is solved by the Newton–Raphson iteration method for Q_{i+1}^{j+1} as

$$\left(Q_{i+1}^{j+1}\right)_{k+1} = \left(Q_{i+1}^{j+1}\right)_k - \frac{f\left(Q_{i+1}^{j+1}\right)}{f'\left(Q_{i+1}^{j+1}\right)} \tag{10}$$

The convergence criterion for the iteration process is

$$\left|f\left(Q_{i+1}^{j+1}\right)_{k+1}\right| \le \varepsilon \tag{11}$$

where $f'(Q_{i+1}^{j+1})$ represents the first derivative of Q_{i+1}^{j+1} and ε is an error criterion.

Explicit–implicit MacCormack schemes

Based on a predictor–corrector–updating three-step procedure (MacCormack 1969, 1985; Tseng & Wang 2004), the first step follows the algorithm as

$$\Delta A_i^p = -\frac{\Delta t}{\Delta x}(Q_{i+1} - Q_i) + q_{l_i}\Delta t \tag{12}$$

$$\left(1 + \lambda\frac{\Delta t}{\Delta x}\right)\delta A_i^p = \Delta A_i^p + \lambda\frac{\Delta t}{\Delta x}\delta A_{i+1}^p \tag{13}$$

$$A_i^p(t + \Delta t) = A_i(t) + \delta A_i^p \tag{14}$$

The correct step follows the algorithm as

$$\Delta A_i^c = -\frac{\Delta t}{\Delta x}(Q_i - Q_{i-1})^p + q_{l_i}^p\Delta t \tag{15}$$

$$\left(1 + \lambda\frac{\Delta t}{\Delta x}\right)\delta A_i^c = \Delta A_i^c + \lambda\frac{\Delta t}{\Delta x}\delta A_{i-1}^c \tag{16}$$

$$A_i^c(t + \Delta t) = A_i(t) + \delta A_i^c \tag{17}$$

where the subscript p and c stand for the predictor and the corrector steps, respectively. The parameter λ is chosen to ensure unconditional linear stability. This requires

$$\lambda = \max\left(0, |c_k| - \frac{\Delta x}{\Delta t}\right) \tag{18}$$

The third step updates the algorithm with the unknown variables of A and Q as follows:

$$A_i(t + \Delta t) = \frac{1}{2}(A_i^p + A_i^c) \tag{19}$$

$$Q_i(t+\Delta t) = \left(\frac{c_I S_o^{1/2}}{nP^{2/3}}\right) A_i^{5/3}(t+\Delta t) \tag{20}$$

In the above equations, the parameter λ is used to represent the IMAC and EMAC schemes in the same formulation. The IMAC and EMAC schemes have second-order accuracy in both time and space. The relations are presented as

$$\left.\begin{array}{l} \lambda = 0 \rightarrow \text{EMAC} \\ \lambda \neq 0 \rightarrow \text{IMAC} \end{array}\right\} \tag{21}$$

For the stability of the EMAC scheme, the CFL condition must be satisfied:

$$\text{CFL} = \frac{\Delta t}{\left[\frac{\Delta x}{u+c}\right]} \leq 1.0 \tag{22}$$

where CFL is the Courant number. For the implicit methods such as the IMAC and INKW schemes, the unconditional stability is the consideration.

NUMERICAL RESULTS AND DISCUSSION

An important test of the quality of a computational model is its ability to reproduce standard test cases or benchmarks. The numerical simulations of overland and open-channel flow benchmark cases are presented. The results are compared with the corresponding analytical solutions in this section. All the simulations were executed on a Toshiba Tablet PC (1.33 GHz CPU, 752 MB RAM).

For the quantitative comparison of the performance characteristics of the numerical schemes, two evaluation indexes are defined by the L_2^m norm and the *Efficiency* index.

The mean relative error is described by the L_2^m norm:

$$L_2^m(\%) = \frac{100}{N}\left[\frac{\sum\left(H_i^{\text{cal}} - H_i^{\text{analytic}}\right)^2}{\sum (H_i^{\text{analytic}})^2}\right]^{1/2} \tag{23}$$

where N is the number of observations, and H_i^{cal} and H_i^{analytic} are the simulated and analytical values at grid point (i), respectively.

The Efficiency index is defined as

$$\text{Efficiency}(\Delta t = X) = \frac{\text{CPU time of } \Delta t_{\min}}{\text{CPU time of } \Delta t = X} \tag{24}$$

Overland flow case

The performance of the proposed numerical method was first tested by computing the overland flow hydrograph associated with uniform rainfall on a parking lot. An effective rainfall continues for 1,500 s with an intensity of 0.1 m/h over a 500 m long and 100 m width parking lot. The slope of the plane is 0.01 and the Manning roughness coefficient is 0.005. The initial condition is a dry bed state.

First, it is important to inspect the behavior of a numerical scheme over a range of grid sizes and time

Table 1 | Sensitivity analysis for test cases using the IMAC scheme

Test cases	Δx (m)	Δt (s)	L_2^m(%) Depth (y)	L_2^m(%) Discharge (Q)	CPU time (s)
Overland flow	25	10	0.0471	0.0781	0.3203
Overland flow	10	5	0.0144	0.0240	0.5195
Overland flow	1	1	2.26×10^{-3}	3.76×10^{-3}	8.4531
Overland flow	1	0.5	3.95×10^{-4}	6.64×10^{-4}	11.937
Channel flow	1,500	50	0.0564	0.0935	0.6289
Channel flow	300	10	9.62×10^{-3}	0.0159	3.1875
Channel flow	30	2	2.81×10^{-3}	4.64×10^{-3}	16.734
Channel flow	30	1	2.35×10^{-3}	3.88×10^{-3}	23.305

increments. A quantitative comparison of the simulated results using the IMAC scheme can be found in Table 1. The analytical solution for the kinematic wave flow with constant rainfall is obtained by Eagleson's solution (1970). The results indicate that the computational error (L_2^m) decreases as the grid size (Δx) or the time increment (Δt) decreases. On the other hand, the computational time increases as the grid size or the time increment decreases. These results clearly show that the proposed IMAC scheme is essentially conservative. This comparison also demonstrates that the proposed IMAC scheme can acquire remarkable accuracy with $\Delta x = 1$ m and $\Delta t \leqq 1$ s, where the L_2^m norms of depth and discharge are both less than 5×10^{-3}%. The time step of 0.5 s leads to a Courant number approximately between 0.9 and 0.5.

Figure 1 compares the simulation results of the water depth, as well as the flow rate, with the analytical solution for the EMAC, IMAC and INKW schemes, respectively. A uniform mesh distribution with 500 cells and a time increment of 0.5 s was used in the computation. As can be seen, the agreement between the analytical solution and the numerical solution is remarkable for both the water depth and the flow rate, except for the INKW scheme. Since the INKW scheme is only a first-order method, significant numerical damping leads to smearing of the peak depth and peak discharge, as shown in the inset graphs. The results of the simulation also indicate that the IMAC and EMAC schemes are slightly better than those of the INKW scheme. Figure 2 demonstrates the simulation result of the water depth using the IMAC scheme with $\Delta t = 1$ s, 10 s, and 100 s, respectively. It can be observed that the simulated hydrograph closely follows the analytical solution, even in the case of a very large time step employed.

As indicated in Table 2, the simulated results of the IMAC and EMAC schemes for the $\Delta x = 1$ m and $\Delta t = 0.5$ s case are identical, except in the aspect of time consumption where the IMAC scheme showed some increase. However, for the cases where $\Delta t \geq 1$ s, the traditional EMAC scheme failed to compute the overland flow. In contrast, the proposed IMAC scheme was able to simulate very well, even in the case where $\Delta t = 100$ s. All the relative errors for the Δt (s) values varying from 0.5 to 100 are less than 0.5%,

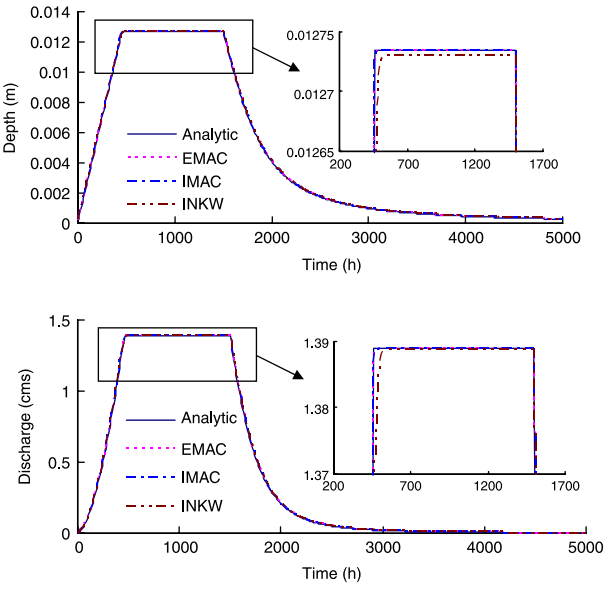

Figure 1 | Solution of overland flow using the EMAC, IMAC and INKW schemes ($\Delta t = 0.5$ s).

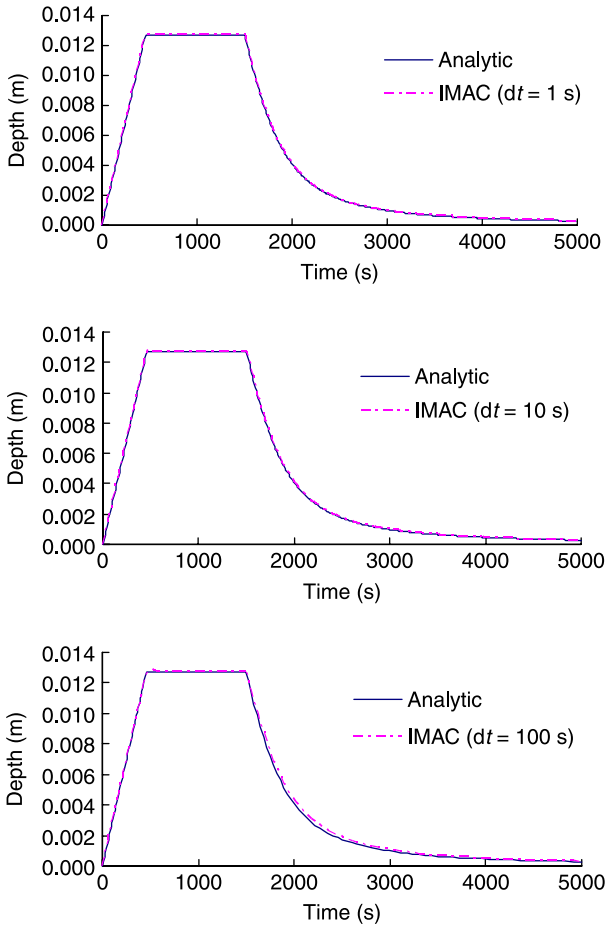

Figure 2 | Simulation hydrograph of depth for overland flow.

Table 2 | Simulation results for the overland flow problem

Schemes	Δx (m)	Δt (s)	L_2^m(%) Depth (y)	L_2^m(%) Discharge (Q)	CPU time (s)	Efficiency
EMAC	1	0.5	3.95×10^{-4}	6.64×10^{-4}	9.5117	1.00
IMAC	1	0.5	3.95×10^{-4}	6.64×10^{-4}	11.937	0.80
EMAC	1	1	N/A	N/A	N/A	N/A
IMAC	1	1	2.26×10^{-3}	3.76×10^{-3}	8.4531	1.13
IMAC	1	5	6.26×10^{-3}	0.0104	3.2539	2.92
IMAC	1	10	0.0176	0.0293	2.1211	4.48
IMAC	1	50	0.1000	0.1652	0.7305	13.02
IMAC	1	100	0.2770	0.4516	0.4805	19.80
INKW	1	0.5	0.0458	0.0775	13.5195	0.70
INKW	1	1	0.0506	0.0855	6.9375	1.37
INKW	1	5	0.0935	0.1561	1.9539	4.87
INKW	1	10	0.1484	0.2456	1.0195	9.33
INKW	1	50	1.182	1.878	0.2695	35.29
INKW	1	100	2.828	4.324	0.1797	52.93

Note: "N/A" = Not Available.

which demonstrates that the proposed IMAC model is accurate, robust and highly stable.

For the higher time increment values, a linear increase in the value of Δt was employed to overcome the difficulty imposed by the initial dry bed condition. The imposed difficulty is apparent when a very large initial time step was used. The CPU times required for the EMAC scheme ($\Delta t = 0.5$ s), the IMAC scheme ($\Delta t = 10$ s) and the IMAC scheme ($\Delta t = 100$ s) are 9.5117 s, 2.1211 s and 0.4805 s, respectively. The Δt value is an indicator of the efficiency of the numerical scheme, the value of which increases with the efficiency of the numerical scheme. As shown in Table 2, the values of the *Efficiency* index for the EMAC scheme ($\Delta t = 0.5$ s), the IMAC scheme ($\Delta t = 10$ s) and the IMAC scheme ($\Delta t = 100$ s) are 1.00, 4.48 and 19.80, respectively. The results clearly indicate that the proposed IMAC scheme, which allowed the use of time steps of magnitudes bigger than those in the EMAC scheme, is a very robust algorithm which can be used to calculate the unsteady overland flow.

Table 2 also enumerates the simulation results for the overland flow problem using the INKW scheme. It is apparent that the INKW scheme appears to be more efficient than the IMAC scheme. However, the levels of accuracy are lower in magnitude than those of the IMAC scheme. Since the INKW scheme has only a first-order accuracy, the resulting computation time is slightly less than that of the second-order scheme (IMAC).

Channel flow case

The above benchmark problem only tests the proposed approach to simulate transient overland flow. In this subsection, we demonstrate the capability of the proposed model to describe an unsteady channel flow. In order to do this, a flood event over a 1500-foot-long, 200-foot-wide rectangular channel with a bed slope of 0.01, and a Manning roughness coefficient of 0.035, was simulated to compute the outflow hydrograph. The initial condition was a uniform flow of 2,000 cfs along the channel. At the upstream boundary, the following hydrograph $Q(t)$ was imposed as

$$\begin{cases} Q(t) = 2000\,\text{cfs} & 0 \le t \le 12\,\text{min} \\ Q(t) = 2000 + \frac{1000}{12}(t-12)\,\text{cfs} & 12 \le t \le 60\,\text{min} \\ Q(t) = 6000 - \frac{1000}{12}(t-60)\,\text{cfs} & 60 \le t \le 108\,\text{min} \\ Q(t) = 2000\,\text{cfs} & 108 \le t \le 150\,\text{min} \end{cases} \tag{25}$$

The simulated outflow hydrograph of water depth at the downstream of the channel using the IMAC scheme

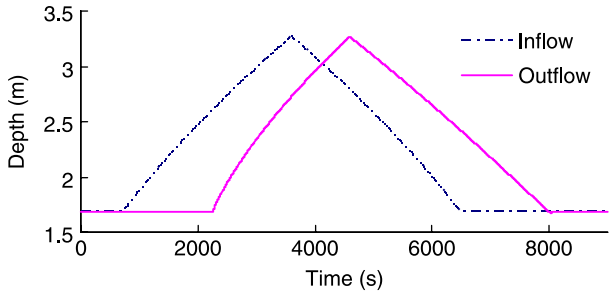

Figure 3 | Inflow and outflow hydrographs using the IMAC scheme ($\Delta t = 2$ s).

with $\Delta x = 30$ ft and $\Delta t = 2$ s is given in Figure 3. The simulation result indicates that the total areas under the hydrographs are almost identical. In other words, the proposed scheme can conserve the total water mass when the flood wave passes through the channel reach. The simulation results evidently reveal that the kinematic wave

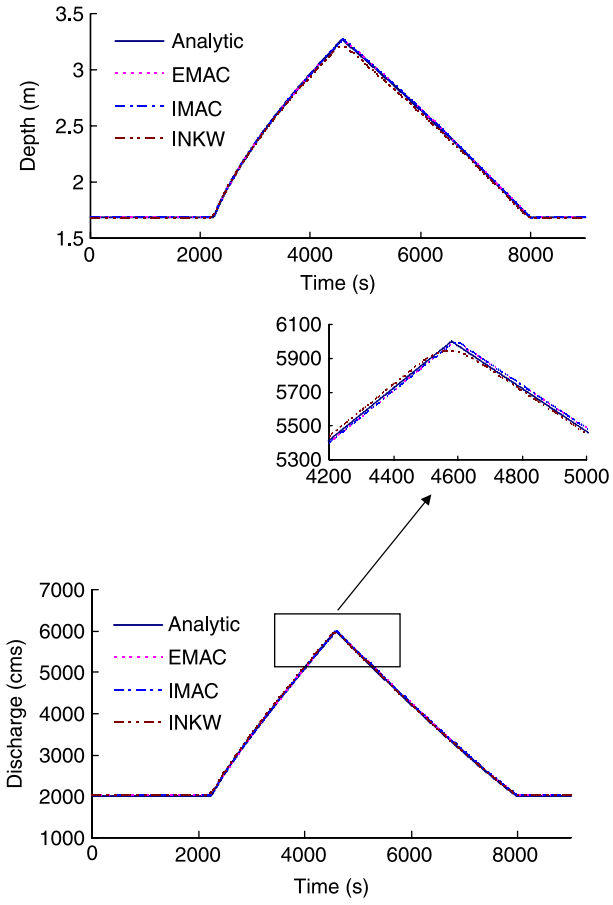

Figure 4 | Solution of channel flow using the EMAC, IMAC and INKW schemes ($\Delta t = 1$ s).

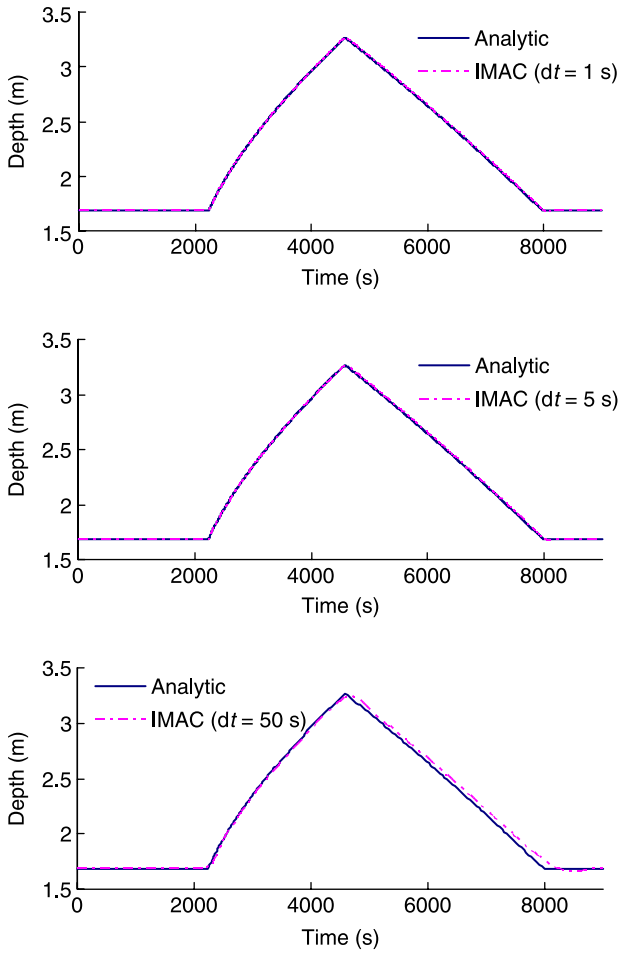

Figure 5 | Simulation hydrograph of depth for channel flow.

does not subside or disperse, but changes its shape because its velocity depends upon the depth (Chou *et al.* 1988).

Table 1 also shows the behavior of the IMAC scheme over a range of grid sizes and time increments for the channel flow case. The analytical solution for kinematic wave channel flow can be obtained by simultaneously solving the characteristic Equations (7) and (8). These results indicate that the computational error (L_2^m) decreases as the grid size (Δx) or the time increment (Δt) decreases. On the other hand, the computational time increases as the grid size or the time step decreases. These results clearly verify that the proposed IMAC scheme is conservative. This comparison also evidently demonstrates that the proposed IMAC scheme can acquire remarkable accuracy with $\Delta x = 30$ m and $\Delta t \leqq 2$ s, where both the L_2^m norms of depth and discharge are less than

5×10^{-3}%. The time increment of 1 s leads to a Courant number approximately between 0.9 and 0.5.

Figure 4 compares the simulation results of the water depth, as well as the flow rate, with the analytical solution for the EMAC, IMAC and INKW schemes, respectively. A uniform mesh distribution of 500 cells and time step of 1 s was used in the computation. As can be seen, an excellent match between the analytical solution and the numerical solution is notable for the EMAC and IMAC schemes. Since the INKW scheme has only a first-order accuracy, significant numerical damping leads to smoothing of the peak depth and peak discharge, as seen in the inset. The results of simulation also indicate that the IMAC and EMAC schemes are slightly better than the INKW scheme. Figure 5 illustrates the simulation result of the water depth using the IMAC scheme with $\Delta t = 1$ s, 5 s and 50 s, respectively. It can be observed that the simulated hydrograph closely follows the analytical solution even in the case of the very large time step employed. The simulated hydrograph of water depth shows a faster wave movement for the $\Delta t = 50$ s case, but the overall accuracy is still satisfactory.

As indicated in Table 3, the simulated results of the the IMAC scheme are almost identical with the IMAC and EMAC schemes for the $\Delta x = 30$ ft and $\Delta t = 1$ s cases. For the case with $\Delta t \geqq 2$ s, the traditional EMAC scheme failed to compute the channel flow. On the other hand, the proposed IMAC scheme was able to simulate very well even in the case of $\Delta t = 100$ s. All the relative errors for the Δt (s) values varying from 1 to 100 are less than 0.5%, which demonstrates once more that the proposed IMAC model is accurate, robust and highly stable.

To avoid the accumulation of the initial error caused by using a very large initial time step, a linear increase in the value of Δt was employed for the higher time increment values. The CPU times required for the EMAC scheme ($\Delta t = 1$ s), the IMAC scheme ($\Delta t = 10$ s) and the IMAC scheme ($\Delta t = 100$ s) are 22.892 s, 6.1602 s and 1.1211 s, respectively. As shown in Table 3, the values of the *Efficiency* index for the EMAC scheme ($\Delta t = 1$ s), the IMAC scheme ($\Delta t = 10$ s) and the IMAC scheme ($\Delta t = 100$ s) are 1.00, 3.72 and 20.42, respectively. The results evidently prove that the proposed IMAC scheme, which allowed the use of time steps of magnitudes bigger than those in the EMAC scheme, is a very robust algorithm which can be employed to calculate the transient flood wave in steep rivers.

Table 3 also lists the simulation results for the channel flow problem using the INKW scheme. It is shown that the efficiency is nearly the same between the IMAC and INKW

Table 3 | Simulation results for the channel flow problem

Schemes	Δx (m)	Δt (s)	L_2^m(%) Depth (y)	L_2^m(%) Discharge (Q)	CPU time (s)	Efficiency
EMAC	30	1	2.35×10^{-3}	3.88×10^{-3}	22.892	1.00
IMAC	30	1	2.35×10^{-3}	3.88×10^{-3}	23.305	0.98
EMAC	30	2	N/A	N/A	N/A	N/A
IMAC	30	2	2.81×10^{-3}	4.64×10^{-3}	16.734	1.37
IMAC	30	5	3.99×10^{-3}	6.59×10^{-3}	9.4141	2.43
IMAC	30	10	6.12×10^{-3}	0.0101	6.1602	3.72
IMAC	30	50	0.0309	0.0512	1.9922	11.49
IMAC	30	100	0.0717	0.1192	1.1211	20.42
INKW	30	1	0.0101	4.89×10^{-3}	80.467	0.28
INKW	30	2	0.0143	7.30×10^{-3}	39.848	0.57
INKW	30	5	0.0230	0.0137	17.004	1.35
INKW	30	10	0.0335	0.0245	9.0625	2.53
INKW	30	50	0.0994	0.1303	1.7422	13.14
INKW	30	100	0.1880	0.2883	0.9414	24.32

Note: "N/A" = Not Available.

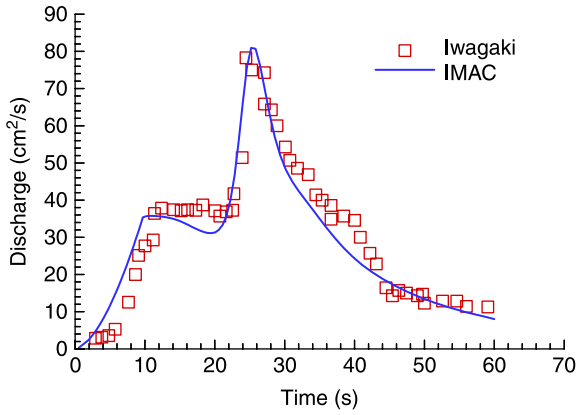

Figure 6 | Discharge hydrograph for flow over three-plane cascade with rainfall duration of 10 s.

schemes. However, the accuracy is almost a magnitude lower than that in the IMAC scheme. Since the INKW scheme only has first-order accuracy, the computation accuracy is significantly less than that of the second-order scheme (IMAC).

Overland flow over a three-plane cascade surface

The above test cases only compared the simulation with analytical solutions and results of other schemes. To illustrate that the proposed model is capable of describing real rainfall–runoff scenarios, the model prediction is compared with the laboratory experiments of Iwagaki (1955). The experiments were conducted to simulate rainfall–runoff processes over a three-plane cascade surface. A series of

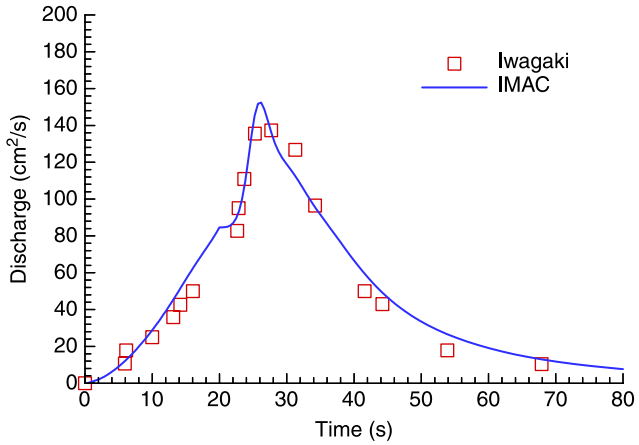

Figure 7 | Discharge hydrograph for flow over three-plane cascade with rainfall duration of 20 s.

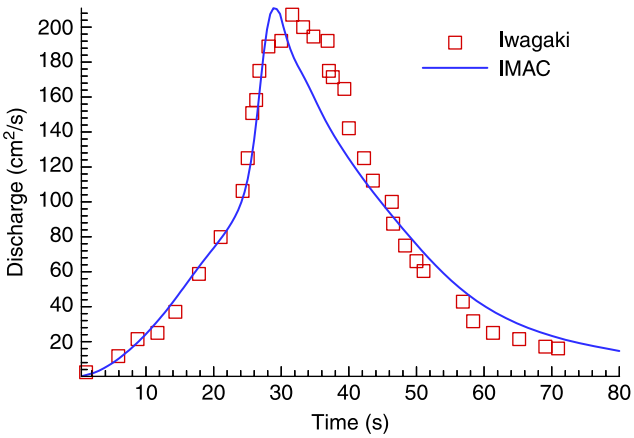

Figure 8 | Discharge hydrograph for flow over three-plane cascade with rainfall duration of 30 s.

artificial rainfall was applied on a smooth aluminum laboratory flume surface. The flume is 24 m in length and is divided into three planes with constant slopes of 0.020, 0.015 and 0.010, respectively, from upstream to downstream. The constant rainfall intensities of 389, 230 and 288 cm/h were applied to the upper, middle and lower plane, respectively, for durations of 10 s, 20 s and 30 s in three experiments.

The flow domain is discretized into 97 grids with a uniform grid spacing $\Delta x = 0.25$ m and the Courant number CFL = 5.0. Manning coefficients of 0.085, 0.011 and 0.013 were employed for the three test simulations, respectively. The computed outflow hydrographs compared with experimental data for the three cases are shown in Figures 6–8. The agreement between the prediction and the experimental results is satisfactory. This result compares favorably with those of Borah *et al.* (1980) with a kinematic shock-fitting model, Zhang & Cundy (1989) with the explicit MacCormack finite-difference scheme and Tisdale *et al.* (1998) with the upwind finite element method. Also, it is shown that the proposed IMAC scheme is capable of simulating the kinematic shock waves which were generated by the changes in bed slopes for the cases of short rainfall duration.

CONCLUSIONS

A simple, accurate and efficient kinematic wave numerical model is developed to simulate the one-dimensional overland and open-channel flows by using a family

of MacCormack-type finite-difference schemes, namely the explicit MacCormack (EMAC) scheme and the implicit MacCormack (IMAC) scheme. The accuracy, efficiency and robustness of the proposed model were verified with two analytical solutions and one experimental measurement for transient overland and open-channel flows. The verifications produced relevant data agreements. These simulated results demonstrated that the proposed IMAC model exhibited high accuracy and robust stability.

Comparisons with the traditional EMAC model showed that a new feature has been enhanced in the proposed model. Based on a direct extension of the EMAC scheme, an implicit correction step was added to offset the restriction of the usual CFL stability condition. Furthermore, the computation efficiencies of the IMAC scheme increased approximately 20 times faster than those of the EMAC scheme for both the overland and channel flows. In comparison with the implicit nonlinear kinematic wave (INKW) scheme, it was shown that the INKW scheme seemed slightly more efficient than the IMAC scheme. However, the accuracy of the former appeared almost a magnitude lower than that of the IMAC scheme.

Based on the results of this study, the IMAC scheme is the best choice for the simulation of kinematic waves flow in overland and open-channel cases. This scheme can allow the use of time steps of larger magnitudes than those in the explicit schemes. Likewise, the scheme achieved a second-order accuracy in space and time. In addition, the IMAC scheme can remain stable and accurate, provided that the CFL does not become too large to prevent the calculation of the time-dependent problems. In other words, the IMAC scheme has a bidiagonal nature that could allow the explicit evaluation of additional implicit corrections. In short, the IMAC scheme does not require a lot of computational effort. This contributes to the simplicity, accuracy and efficiency of the proposed model.

ACKNOWLEDGEMENTS

A portion of this work was supported by the National Science Council, ROC, under grant no. NSC-97-2211-E-040-007. This support is greatly appreciated.

REFERENCES

Borah, D. K., Prasad, S. N. & Alonso, C. V. 1980 Kinematic wave routing incorporating shock fitting. *Water. Resour. Res.* **16**, 529–541.

Chou, V. T., Maidment, D. R. & Mays, L. W. 1988 *Applied Hydrology*. McGraw-Hill, New York.

Cundy, T. W. & Tento, S. W. 1985 Solution to the kinematic wave approach to overland flow routing with rainfall excess given by the Philip equation. *Water. Resour. Res.* **21**, 1132–1140.

Cunge, J. A., Holly, F. M. & Verwey, A. 1980 *Practical Aspects of Computational River Hydraulics*. Pitman, London.

Freeze, R. A. 1978 Mathematical models of hillslope hydrology. In *Hillslope Hydrology* (ed. in M. J. Kirkby), pp. 177–225. Wiley Interscience, New York.

Henderson, F. M. 1966 *Open Channel Flow*. MacMillan, New York.

Iwagaki, Y. 1955 *Fundamental Studies on Runoff Analysis by Characteristics*. Bulletin 10, Disaster Prevention Research Institute, Kyoto University, pp. 1–25.

Kazezyılmaz-Alhan, C. M., Medina, M. A. & Rao, P. 2005 On numerical modeling of overland flow. *Appl. Math. Comput.* **166**, 724–740.

Li, R. M., Simons, D. B. & Stevens, M. A. 1975 Nonlinear kinematic wave approximation for water routing. *Water. Resour. Res.* **11** (2), 245–252.

Lighthill, M. J. & Witham, G. B. 1955 On kinematic waves 1: flood movement in long rivers. *Proc. R. Soc. A* **229**, 281–316.

MacCormack, R. W. 1969 *Effect of viscosity in hypervelocity impact cratering*. AIAA Paper 69–354.

MacCormack, R. W. 1985 *Current status of numerical solutions of the Navier–Stokes Equations*. AIAA Paper 85–32.

Singh, V. P. 1996 *Kinematic Wave Modeling in Water Resources: Surface Water Hydrology*. Wiley, New York.

Tisdale, T. S., Scarlatos, P. D. & Hamrick, J. M. 1998 Streamline upwind finite-element method for overland flow. *J. Hydraul. Eng.* **124**, 350–357.

Tseng, M. H. & Chu, C. R. 2000 Simulation of dam-break flow by an improved predictor-corrector TVD. *Adv. Water. Resour.* **23**, 637–643.

Tseng, M. H. & Wang, S. S. Y. 2004 One-dimensional channel flow simulations with irregular bed topography. *J. Chinese Inst. Civil Hydraul. Eng.* **16** (2), 211–218.

Zhang, W. & Cundy, W. 1989 Modeling of two-dimensional overland flow. *Water. Resour. Res.* **25**, 2019–2035.

First received 26 September 2008; accepted in revised form 11 June 2009. Available online 7 January 2010